Landslide characteristics and spatial distribution in the Rwenzori Mountains, Uganda

Liesbet Jacobs [a, b, *], Olivier Dewitte [b], Jean Poesen [c], Jan Maes [a, c], Kewan Mertens [d], John Sekajugo [e], Matthieu Kervyn [a]

[a] Vrije Universiteit Brussel, Department of Geography, Earth System Science, Pleinlaan 2, 1050 Elsene, Belgium
[b] Royal Museum for Central Africa, Department of Earth Sciences, Leuvensesteenweg 13, 3080 Tervuren, Belgium
[c] KU Leuven, Division of Geography and Tourism, Celestijnenlaan 200E, 3001 Heverlee, Belgium
[d] KU Leuven, Division of Bio-economics, Celestijnenlaan 200E, 3001 Heverlee, Belgium
[e] Busitema University, Department of Natural Resource Economics, P.O. Box 236, Tororo, Uganda

ARTICLE INFO

ABSTRACT

In many landslide-prone regions, data on landslide characteristics remain poor or inexistent. This is also the case for the Rwenzori Mountains, located on the border of Uganda and the DR Congo. There, landslides frequently occur and cause fatalities and substantial damage to private property and infrastructure. In this paper, we present the results of a field inventory performed in three representative study areas covering 114 km². A total of 371 landslides were mapped and analyzed for their geomorphological characteristics and their spatial distribution. The average landslide areas varied from less than 0.3 ha in the gneiss-dominated highlands to >1 ha in the rift alluvium of the lowlands. Large landslides (>1.5 ha) are well represented while smaller landslides (<1.5 ha) are underrepresented. The degrees of completeness of the field inventories are comparable to those of similar historical landslide inventories. The diversity of potential mass movements in the Rwenzori is large and depends on the dominant lithological and topographic conditions. A dominance of shallow translational soil slides in gneiss and of deep rotational soil slides in the rift alluvium is observed. Slope angle is the main controlling topographic factor for landslides with the highest landslide concentrations for slope angles above 25−30° in the highlands and 10−15° in the lowlands. The undercutting of slopes by rivers and excavations for construction are important preparatory factors. Rainfall-triggered landslides are the most common in the area, however in the zones of influence of the last two major earthquakes (1966: Mw = 6.6 and 1994: Mw = 6.2), 12 co-seismic landslides were also observed.

1. Introduction

The construction of landslide inventories and the investigation of their typologies and spatial distributions are indispensable tools for unravelling landslides' spatial and temporal signatures. This contributes to understanding landscape evolution and determining landslide susceptibility and hazard. Consequently, landslide risk reduction is not possible without this first assessment (Crozier and Glade, 2005). Despite the general recognition of their importance, landslide inventories are scarce with globally only 1% of the slopes on landmasses covered by landslide maps (Guzzetti et al., 2012).

On the African continent, this systematic under-documentation of landslides is even more pronounced especially when considering scientific literature. In spite of their socio-economic impacts, landslides are only rarely studied (Maes et al., accepted with revision). In literature, few examples exist of reported landslides there (e.g. Davies, 1996; Ayalew, 1999; Ngecu and Ichangi, 1999; Zogning et al., 2007) and systematic landslide inventories in sub-Sahara Africa are particularly rare (e.g. Knapen et al., 2006; Van Den Eeckhaut et al., 2009; Che et al., 2011; Maki Mateso and Dewitte, 2014). This is also true for the Rwenzori Mountains, where landslides have claimed over 30 lives in the past 15 years, displaced several thousands of people and caused severe damage to crops, livestock, infrastructure and road networks (Jacobs et al., 2015; Mertens et al., 2016). Despite these destructive impacts,

* Corresponding author. Vrije Universiteit Brussel, Department of Geography, Earth System Science, Pleinlaan 2, 1050 Elsene, Belgium.
E-mail address: liesbet.jacobs@vub.ac.be (L. Jacobs).

systematic mapping or geomorphological characterization of these landslides is currently lacking.

In this paper we describe the results of a field inventory of landslides covering diverse lithological and geomorphological units within the Rwenzori Mountains. This inventory, which includes the geomorphological description of landslides and their spatial distribution, represents a first step in moving towards a landslide hazard analysis and risk reduction strategy for this equatorial highland region.

2. Study area

The Rwenzori Mountains lie on the border of DR Congo and Uganda. They cover an area of ca. 3000 km^2 and reach an altitude of 5109 m a.s.l. (Fig. 1). Due to its unique geomorphological features, its tectonic character, the bio-diversity of its ecosystems and the presence of glaciers on its highest peaks, this asymmetric horst mountain has been the subject for research in various disciplines. A full description of the horst mountain's topography, lithology, soils, climate and seismic activity can be found in Jacobs et al. (2015). Within this horst mountain, we focus on three study areas covering ca.114 km^2 in total. Before the selection of these study areas, preliminary field surveys in several regions of the Rwenzori were conducted to identify areas of landslide concentration. We also considered the zones of landslide concentration indicated by local stakeholders, such as policy-makers and civil society workers, during workshops organized in the three districts of the Rwenzori (Kervyn et al., 2015). In addition, the study areas were selected based on the results from a landslide inventory using archives (Jacobs et al., 2015). A final criterion for the selection was to encompass as much as possible contrasting topographic, climatologic, lithologic and seismic conditions. The study areas are hereafter called Bundibugyo, Kabonero and Mahango based on the main sub-counties or districts covering these areas (Fig. 1). The side of the Rwenzori located in DR Congo is sparsely inhabited and more difficult to access, consequently all study areas are located in Uganda. No study areas are located above 2300 m a.s.l. (the central part of the horst mountain) because here there are no settlements. Due to presence of a national park, this area is not freely accessible. Details of the three study areas are summarized in Table 1.

The Kabonero study area is located in the east of the Rwenzori Mountains (Fig. 1). The study area is bordered by rivers: Yeriyo in the north and Ruigo and Ruimi rivers in the south (Fig. 2). To the west, the national park forms the boundary while to the east the study area ends in the lowlands (starting at 1500 m a.s.l., Fig. 1). The dominant lithologies are amphibolites in the south and gneiss in the north, separated by a small strip of mica schists (Fig. 2) (GTK Consortium, 2012). This region is drier than the other two study areas (Jacobs et al., 2015; Thiery et al., 2015). The Ruimi-Wasa fault borders this region in the East (Fig. 1) which is situated in the most seismically active part of the horst mountain (Lindenfeld et al., 2012). The Kabonero study area is situated at a distance of only 30 and 15 km of the 1966 (Mw = 6.6) and 1994 (Mw = 6.2) earthquake epicenters, respectively. Furthermore, the epicenters of 9 earthquakes with Mw > 4 occurring in the period 1983–2015 are situated within a buffer of 10 km around the study area (USGS, 2015).

The Mahango study area is delimited by the administrative boundary of the Mahango Sub-County (Fig. 1). Topographically, this region is very similar to Kabonero (average elevation of 1730 m a.s.l. and average slope angle of 20°) but extends only in Gneiss (GTK Consortium, 2012) (Fig. 2). This area was selected mainly because of the frequent occurrence of lethal landslides reported in the media (Jacobs et al., 2015). Compared to the dry climate of the north-east part of the Rwenzori, the frequency of intense rainfalls is

higher in Mahango. It is however still less humid than the west and north-west parts (Jacobs et al., 2015; Thiery et al., 2015). The Mahango area is seismically less active than Kabonero according to Lindenfeld et al. (2012) and USGS (2015). The epicenter of the nearest major earthquake (Mw > 5.5, 1994) lies ca. 50 km from the study area's center. Only two earthquakes with Mw > 4 in the period of 1952–2015 occurred within a 10 km buffer from the study area according to the USGS archive (2015).

The Bundibugyo study area lies in the north-west of the Rwenzori and is bordered by the national park in the south. It is also bordered by the Humya and Kirumya rivers and by the Fort Portal-Bundibugyo road in the north (Figs. 1 and 2). This area also includes lowlands of the graben, i.e. at lower elevations (<1000 m a.s.l.) with generally less steep slopes averaging 9°. Here thick accumulations of Pleistocene to Holocene rift alluvium are found (GTK Consortium, 2012). Based on the first general field survey in the region and interviews with local stakeholders, it was found that those lithologies were very prone to landsliding. The study area has a lower average altitude of 1230 m a.s.l. and a smaller average slope angle of 14°. The upper regions of the study area, i.e. above ~1100 m a.s.l., are dominated by gneiss. The rift alluvium and gneiss are separated by a narrow strip of mica schists with quartzitic interbeds (GTK Consortium, 2012) (Fig. 2). This study area receives more precipitation than Mahango and Kabonero (Jacobs et al., 2015; Thiery et al., 2015). Although it is less seismically active than the Kabonero study area, the epicenters of the two last major earthquakes in the Rwenzori (1966: Mw = 6.6 and 1994: Mw = 6.2) lie within a radius of only 30 km to the center of this study area.

3. Materials and methods

3.1. Landslide inventories; types, processes and characteristics

Often landslide inventories are constructed using remote sensing techniques or aerial photographs (Guzzetti et al., 2012). However, due to rapid vegetation regrowth and frequent cloud cover in the humid tropics, the use of these optical techniques is seriously hampered. Although time-consuming, field surveys allow to establish reliable landslide inventories in these conditions.

All landslides -regardless of their age-are considered to construct the multi-temporal landslide inventories. For most landslides GPS points at the head or in the depletion zone of the slide are taken. For some landslides however, an observation from a distance had to be made given the inaccessibility of the terrain. Google Earth imagery (2015) is used wherever possible to assist in mapping landslides if estimates of landslide geometry were difficult, i.e. for landslides mapped from a distance or if vegetation regrowth did not allow good observations.

Each landslide is described in the field to allow classification according to Cruden and Varnes (1996) and Hungr et al. (2014). This inventory protocol includes the following parameters and is constructed to allow landslide mapping by a single person in poorly accessible areas (Table 2):

Using observations on recent activities in the slide body or on (secondary) scarps and discussions with local guides/inhabitants, the activity of the landslide is assessed. A slide is considered active if activity occurred within the past 5 years.

The landslide dimensions are analyzed in a GIS environment. In general assessing the depth of the landslides is a challenge in all study regions due to the inaccessibility of the terrain, the rapid recolonization of the slide by vegetation and the reclamation of the landslide for agriculture. The landslide densities are calculated in #slides/km^2 and in percentage of area covered by landslides.
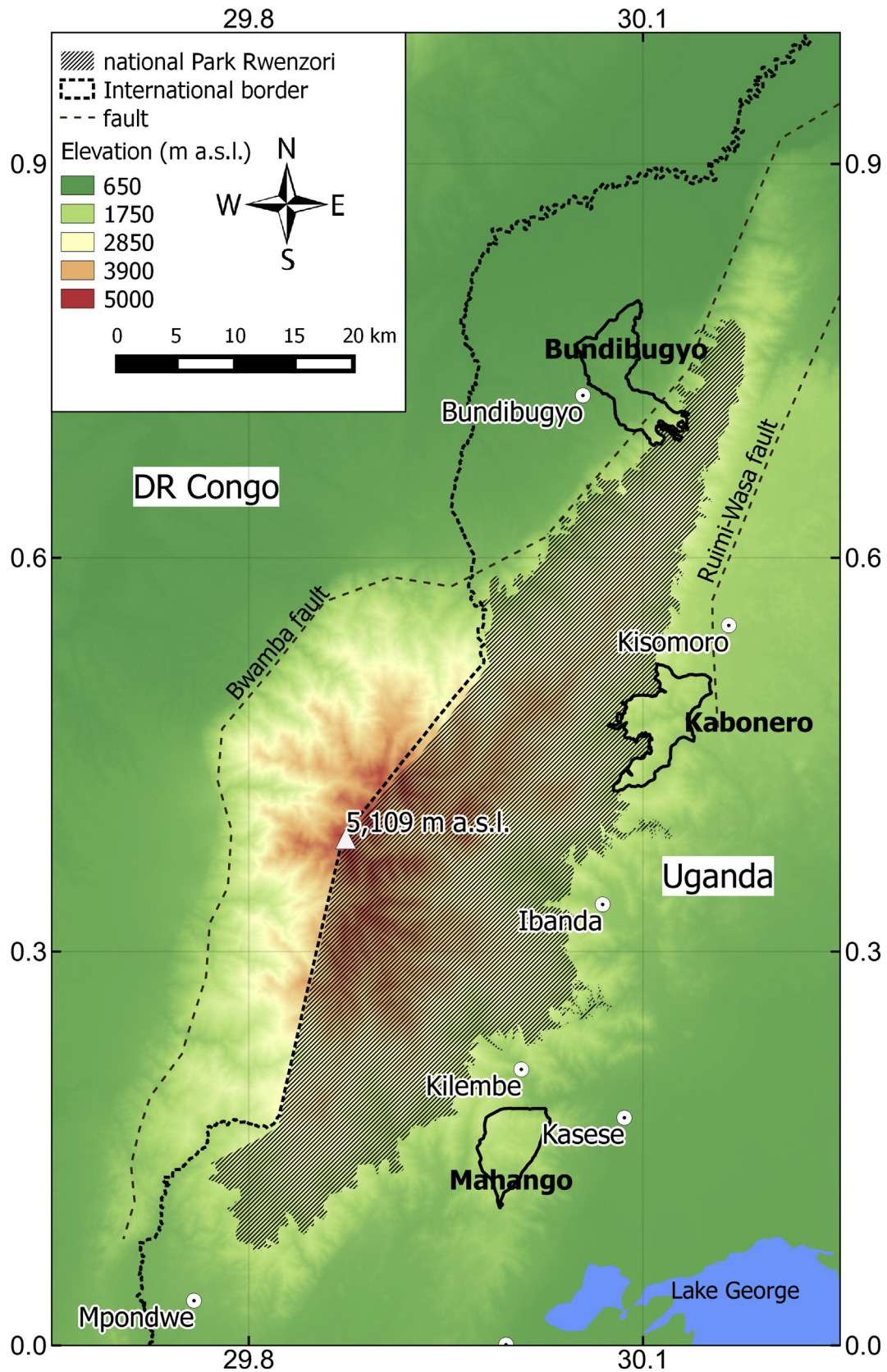
Fig. 1. The Rwenzori Mountains and the three selected study areas (Source of topographic data: Shuttle Radar Topography Mission (SRTM) 1" (USGS, 2014); the boundary of the national park is taken from the AfriCover database (FAO, 2003); source fault location: Lindenfeldt et al., 2012)).

Table 1
Summary of the characteristics of the study areas in the Rwenzori. NA = not applicable.

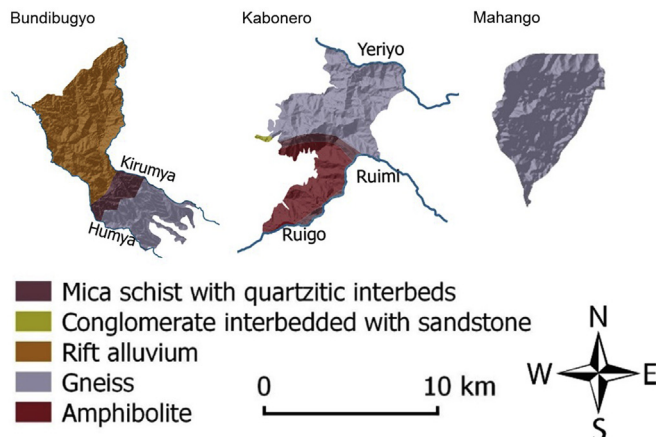| Study area	Area (km^2)	Elevation range (m a.s.l.)	Average slope angle (°)	Lithology	Number of landslides
Kabonero	41	1400–2300	20	gneiss, amphibolite	91
Mahango	30	1240–2200	20	gneiss	70
Bundibugyo	43	715–2200	14	rift alluvium, gneiss	210
Total	**114**	**NA**	**NA**	**NA**	**371**

Fig. 2. Lithology of the three study areas and their lithological units according to GTK Consortium (2012).

potential incompleteness of the landslide inventories (Stark and Hovius, 2001; Malamud et al., 2004; Van Den Eeckhaut et al., 2007). Here, our analysis is based on the probability density function using the three-parameter inverse-gamma probability distribution formulated by Malamud et al. (2004) for complete inventories:

$$p(A_L; \rho, a, s) = \frac{1}{a\Gamma(\rho)}\left[\frac{a}{A_L - s}\right]^{\rho+1}\exp\left[-\frac{a}{A_L - s}\right] \quad (1)$$

with A_L the landslide area (km^2), ρ a parameter determining the exponential decay after the rollover, a the parameter controlling the location of the maximum probability distribution and s the parameter controlling the exponential rollover for small landslides. The negative exponential decay is then defined by $\rho + 1$. Because for historical inventories the total number of landslides in the inventory (N_{LT}) is not known, the probability density function in Eq. (1) cannot be calculated directly (Malamud et al., 2004; Van Den

Table 2
Landslide attributes and physical characteristics identified on the field.

Type	Characteristic	Descriptor
Geometry of the slide	Depth of main scarp	m
	Width of main scarp	m
	Plan shape of scarp	circular/rectilinear
	Estimated length of run-out	m
Material	Type of material moved	Rock/debris/soil
	Bedrock reached	Y/N
Topography of the slide	Presence of reverse slope(s)	Y/N + location
	Presence of springs or stagnating water	Y/N + location
	Presence of drainage lines (or impeded drainage)	Y/N
	Presence of flow patterns	Y/N
	Presence of secondary scarps	Y/N + location
Activity of the slide	Recent activity on main scarp	Y/N
	Recent activity on secondary scarps	Y/N
	Recent activity in slide body	Y/N
	Vegetation in head/middle/base of landslide	type + percentage cover
Triggering factors	Timing of landslide, timing of reactivation	date
	Reports of heavy rainfall before occurrence	Y/N
	Reports of earthquake activity before occurrence	Y/N
Preparatory factors	Road cut	Y/N + type of road + location of contact
	River undercutting	Y/N

3.2. Completeness of the landslide inventory

The establishment of historical (or multi-temporal) landslide inventories is challenging because the landslides are -to different extents-erased by water- or tillage erosion, converted into agricultural land or natural vegetation (Guzzetti et al., 2012). Therefore, especially in the humid tropics, it is useful to check the completeness of multi-temporal inventories. This allows to estimate the quality of the data and gives an idea about the number and area of the slides missing in the inventory. Finally, it enables comparison with other landslide inventories in different settings (Malamud et al., 2004).

Frequency-size distributions are commonly applied to identify

Eeckhaut et al., 2007). To infer about the completeness of such landslide inventories, we need to use the frequency density which is defined by multiplying the probability density with N_{LT} (Malamud et al., 2004). The empirical frequency density distributions for the inventories in the Rwenzori are therefore compared to the theoretical frequency density curve by Malamud et al. (2004) for different total numbers of landslides. To allow this, Malamud et al. (2004) proposed a landslide magnitude scale $m_L = \log_{10}(N_{LT})$. The comparison of the empirical frequency density distribution to the calibrated curves by Malamud et al. (2004) allows the identification of an equivalent m_L. From this, the quantification of missing landslides and missing landslide areas in the field inventories is enabled. A detailed description of this

methodology can be found in Malamud et al. (2004) and Van Den Eeckhaut et al. (2007).

3.3. Controlling, preparatory and triggering factors

We consider (1) controlling factors for the occurrence of landslides (or the preconditions) which determine slope stability and are mostly static in time; (2) preparatory factors which are dynamic in time and prepare the slope for failure and (3) triggering factors which actually trigger the slide (Glade and Crozier, 2005).

To infer about the controlling factors, it is important to select appropriate spatial information on landslide initiation locations. For this purpose, a distinction is made between accumulation and depletion zones for each landslide as defined by Cruden and Varnes (1996). The depletion zone is considered to be the approximate source area of the slide. Based on field observations, this depletion zone is defined as the upper third of the slide, except when the location of the reverse slope is known: in these cases the start of the reverse slope is considered to mark the distinction between depletion and accumulation zones. The centroid of this depletion zone is calculated to represent each landslide, in order to allow for an equal treatment of all landslides regardless of their size (Goetz et al., 2015). The lithological map (GTK Consortium, 2012) and the SRTM 1″ DEM (USGS, 2014) are used to assign a lithology class, slope angle, plan- and profile curvature and slope aspect to the landslide points selected within the depletion zone. Landslides have the potential to alter local slope angle, therefore pre-slide slopes are often calculated manually by interpolation (e.g. Van Den Eeckhaut et al., 2006). However considering that the smallest dimension of landslides mapped in this case-study is often smaller than a pixel and that most of these landslides occurred after the acquisition of the SRTM in 2000 the direct use of the SRTM 1″ slopes is considered to be reliable. The distribution of the lithology, slope angle, plan -and profile curvature and slope aspect in the landslide points is then further compared to the respective distribution of these variables over the entire study areas. The χ^2-tests are applied to infer about the influence of categorical variables on the occurrence of landslides (e.g. Dewitte et al., 2010). Where strong correlations between a controlling factor and the occurrence of landslides occur, the Frequency Ratio (FR) is calculated. This is a measure for the clustering of landslides on a certain variable class (Lee and Pradhan, 2007).

For the preparatory factors, the focus lies on short-term factors like slope oversteepening by erosional activity of floods (e.g. Zogning et al., 2007) and human interventions such as deforestation and slope disturbances for construction. For each slide, it was checked whether a river is connected to the toe i.e. where there is potential for slope undercutting by the river. Similarly, it was registered whether the construction of a house or road or other anthropogenic influences preceded the slope failure.

Finally, information on the triggering factors, was obtained through personal communication when the landslide occurred and whether the landslide occurred due to rainfall or due to earthquake activity. Because written reports exist only for recent and major events, the reliability of these orally reported dates must be taken with care. For most slides the identification of the triggering factor was straightforward. However for landslides older than 50 years, the triggering factors sometimes remain unknown.

4. Results

4.1. Typology and characteristics of landslides per study area

In Kabonero, 70 landslides were mapped, compared to 91 in Mahango and 210 in Bundibugyo (Fig. 3). Landslide densities are summarized in Table 3. In Bundibugyo, maximum densities are almost twice as high as in the two other two study regions and the percentage area covered by landslides over two to four times higher. This high landslide density in Bundibugyo is mostly due to the large number of landslides and large individual size of landslides mapped in the lowlands of Bundibugyo (see section 4.2). Here landslides are mostly deep-seated slides and cover 5.7% of the study area.

In Table 4 details about the sliding mechanisms and the material moved are given. The inventories are visualized in Fig. 3. In Kabonero, translational soil slides are the most common. In seven cases the material displaced could not be identified due to a complete vegetation re-emergence and inaccessibility of the landslide body. The majority of the landslides were shallow (73%) (Fig. 4A). Deep-seated landslides were less common (23%) and the remaining four percent are unclassified. Among the 70 landslides in this study area, 42 were reported to have first occurred before 2010, 18 slides are reported to have first occurred before the 1990s. This makes Kabonero the study area with the oldest landslides. However, 31 of the landslides in the study area had clear signs of recent activity in either the scarp, toe or body, and were therefore classified as currently unstable.

In Mahango, shallow landslides were most common (76%) compared to deep-seated slides (24%). The dominant sliding mechanism in this region is - similar to Kabonero - shallow, translational soil slides (Table 4 and Fig. 4 B and C). Of the 91 landslides, 32 were considered to be stable i.e. no reported activity in the past 5 years and no clear signs of activity within the landslide scarps or body.

In Bundibugyo 210 landslides were mapped. Deep-seated landslides are more frequent than shallow slides (125 vs. 76). Translational and rotational landslides are almost equally present in the overall study area (n = 90 and n = 88 respectively) (Table 4). However, the vast majority of rotational (n = 82) and deep-seated slides (n = 113) are located in the rift alluvium (Fig. 4 D and E) while shallow and translational slides are much more common in the upland regions of the study area. The dominance of deep-seated landslides in the lowlands is because here, deep profiles without bedrock are occurring. The prevalence of shallow landslides on the highlands of Bundibugyo but also Kabonero and Mahango is due to the presence of shallow soils in the upland region, where the bedrock lies near the soil surface. The deep-seated rotational soil slides in the rift alluvium often create reverse slopes and stagnating water. Because landslide scarps in the rift alluvium are often regressive, many of the landslide scarps were found on the top of the ridges. The majority of slides were active during the past 5 years (n = 157).

4.2. Dimensions of the mapped landslides

The data on slide dimensions is summarized in Table 5. The average landslide size in Bundibugyo is almost four times larger than that in Mahango where the smallest slides are found. Furthermore, within each study area, the large standard deviation indicates a significant variation in individual landslide area. The landslide width to length ratio is higher in Bundibugyo uplands (0.6) and lowlands (0.7) than in Kabonero and Mahango (0.4). Finally, with an average depth of 8 m and a maximum depth of 30 m, landslides are much deeper in Bundibugyo (Fig. 4 D and E) than in Kabonero or Mahango (Table 5; Fig. 4 A, B and C).

4.3. Degree of completeness of the landslide inventory

The frequency density distributions for the three separate study areas is shown in Fig. 5. For Kabonero and Bundibugyo, a slight roll-
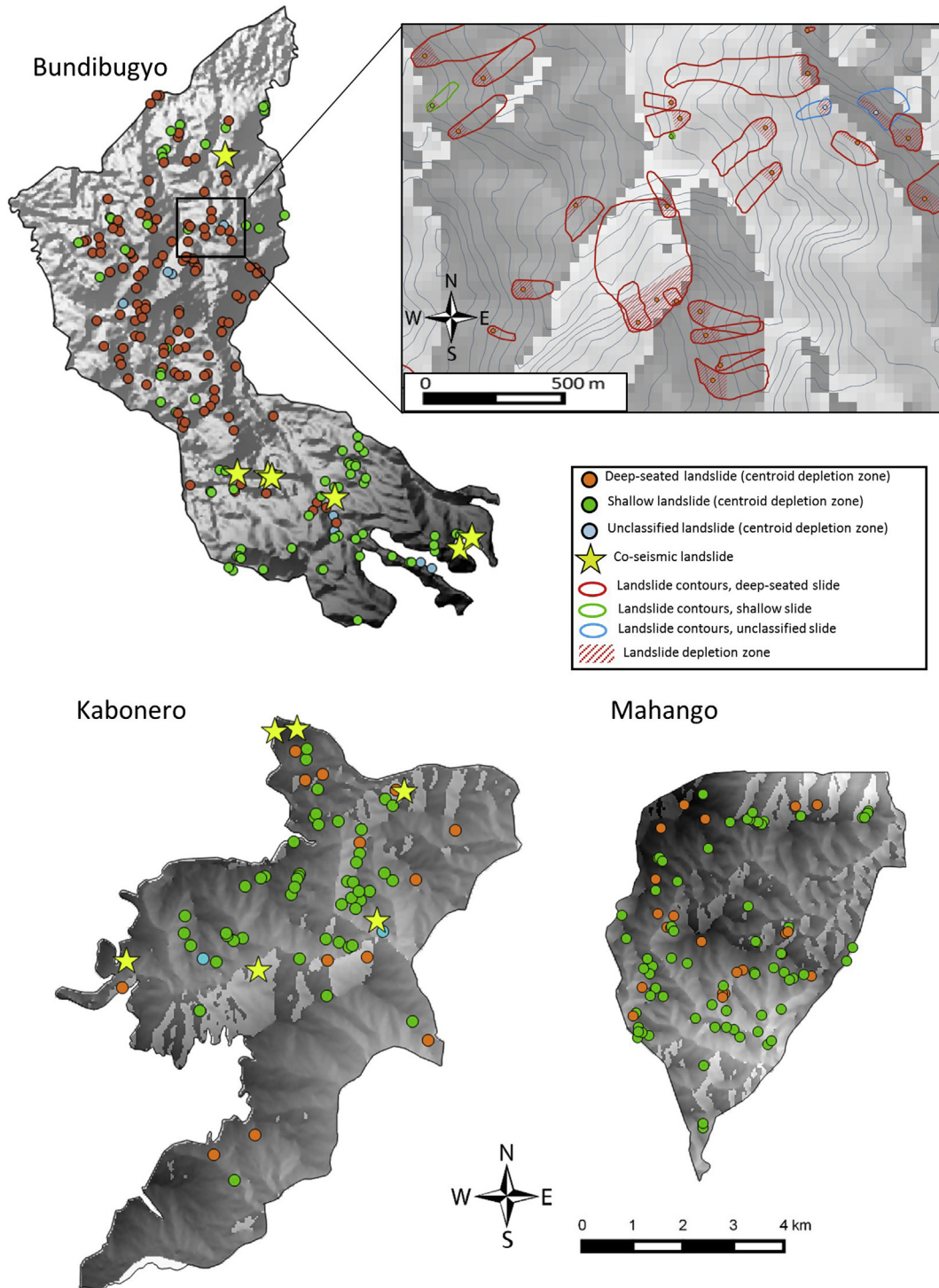
Fig. 3. Landslide inventory maps for the three study areas with detailed zoom.

Table 3
Landslide densities and %area covered by landslides in the three study areas. For total number of landslides and size of study areas, see Table 1.

Study area	Average density (#slides/km²)	Maximum density (#slides/km²)	Average cover (%)
Kabonero	1.7	11	1
Mahango	3.0	11	2
Bundibugyo	4.9	19	5

Table 4
Number of landslides with their sliding mechanisms and material displaced for the three study areas (NA is not available due to dense vegetation regrowth), the boxes indicate the most common landslide type in each study area.

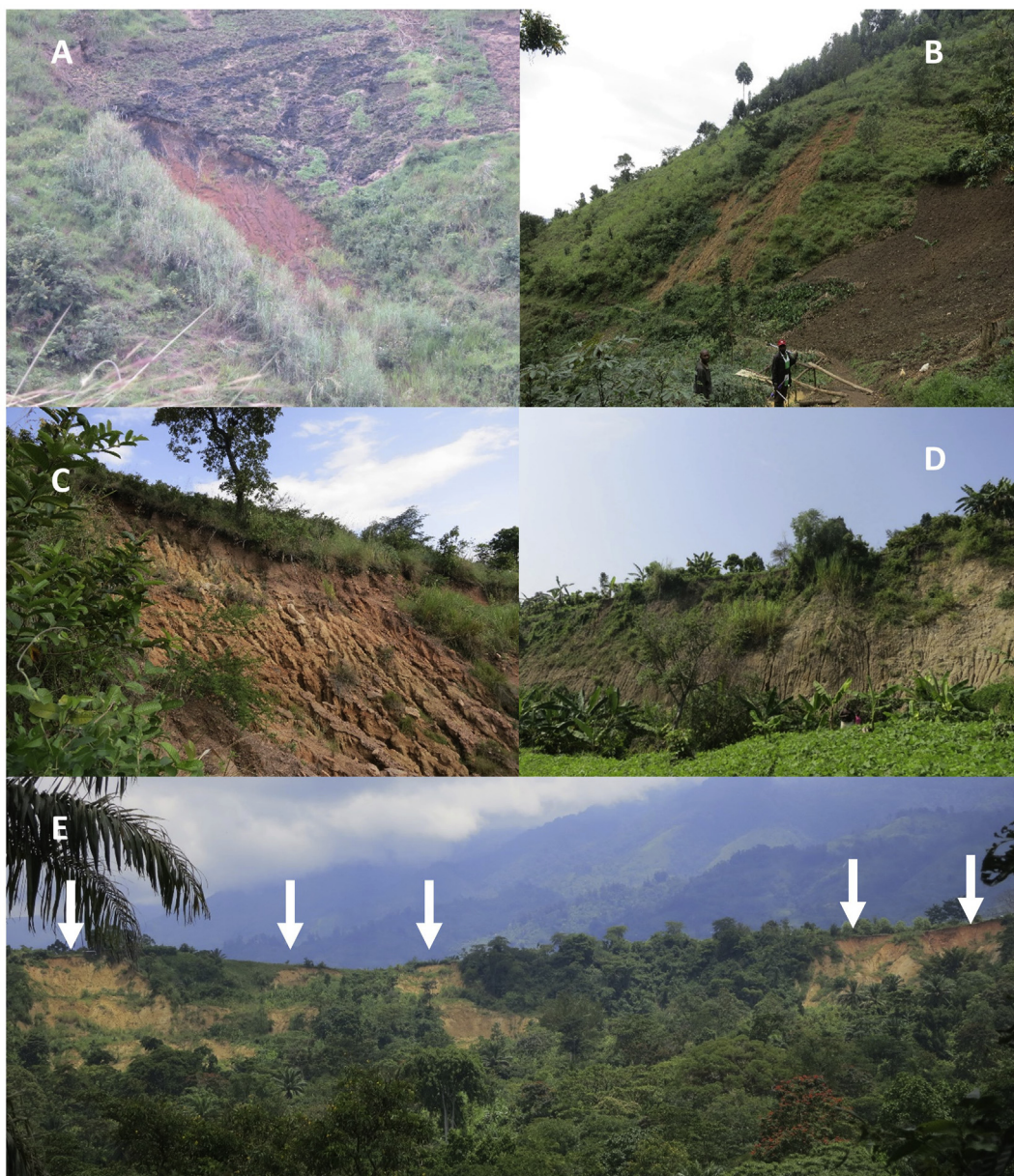|	*Kabonero*				*Mahango*				*Bundibugyo*			
	Displaced material											
Sliding mechanism	*soil*	*debris*	*rock*	*N/A*	*soil*	*debris*	*rock*	*N/A*	*soil*	*debris*	*rock*	*N/A*
Rotational slide	3	0	0	3	7	3	1	1	84	3	0	1
Translational slide	41	7	1	4	55	7	2	5	68	13	1	8
Flow	3	3	0	0	7	2	0	0	2	0	0	0
Complex slides	0	3	0	0	0	0	0	0	0	0	0	0
N/A	2	0	0	0	0	1	0	0	27	1	0	2

Fig. 4. Examples of typical landslides. A: Shallow translational soil slide (Kabonero, August 2014). B: Shallow translational soil slide (Mahango, August 2014). C: Shallow landslide scarp with rill formation and reactivations (Mahango, August 2014). D: Deep-seated rotational soil slide (Bundibugyo, August 2014). E: failed ridge with several deep seated landslides, white arrows indicate head scarps (Bundibugyo, October 2014).

Table 5
Landslide dimensions for the three study areas. n = number of landslides.

| Characteristic	n	Average	Standard deviation	Minimum	Maximum
Kabonero study area					
Landslide area (ha)	54	0.64	1.3	0.012	7.12
Landslide length (m)	56	116	86	18	352
Width main scarp (m)	57	45	51	5	266
Depth main scarp (m)	16	2.3	1.9	0.7	8
Mahango study area					
Landslide area (ha)	74	0.28	0.62	0.0024	5.06
Landslide length (m)	74	98.9	79.8	8	420
Width main scarp (m)	79	30.3	31.2	3	193
Depth main scarp (m)	37	1.7	1.2	0.4	5
Bundibugyo study area					
Landslide area (ha)	156	1.07	1.63	0.019	10.6
Landslide length (m)	158	138	111	10	670
Width main scarp (m)	179	69	66	5	330
Depth main scarp (m)	99	8	7.7	0.3	30
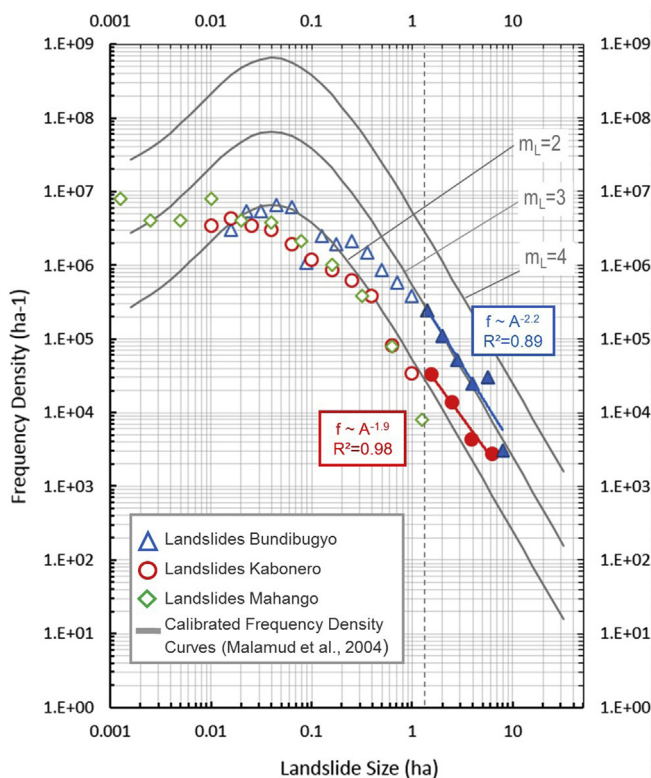
Fig. 5. Frequency density distributions for all landslides mapped in the three study areas plotted with the general landslide frequency density distribution by Malamud et al. (2004) (Eq. (1)) with $\rho = 1.4$, $a = 1.28 \times 10^{-3}$ km^2, $s = -1.32 \times 10^{-4}$ km^2 and m_L from 2 to 4. All landslides are considered including those mapped from a distance and landslides where erosion or vegetation hampered accurate estimations on dimensions. This is justified by the large bin compared to the uncertainty in estimated landslide dimensions. Filled symbols represent landslides larger than 1.5 ha.

over can be observed. For Mahango, the roll-over is not evident. Above landslide sizes of 1.5 ha, the tail of the distributions of Bundibugyo and Kabonero run almost parallel with the frequency density curves for $m_L = 3$ and $m_L = 2.5$ respectively. The rate of exponential decay for landslides above 1.5 ha, is 1.9 ($R^2 = 0.98$) in Kabonero, while in Bundibugyo it is 2.2 ($R^2 = 0.89$). Based on the landslide magnitude scales of $m_L = 2.5$ and $m_L = 3$, the total theoretical number of landslides in Kabonero and Bundibugyo is

calculated to be about 300 and 1000 respectively. Using the theoretical mean landslide area by Malamud et al. (2004), the theoretical total landslide area is calculated. The total number of mapped landslides lies below one fourth of the theoretical total and concerning landslide area, 43–67% of the theoretical total is mapped (Table 6). The obtained distribution for Mahango seems to follow the frequency density distribution for $m_L = 2$, however for very small landslides, the frequency density lies much higher than this curve. Because the equivalent m_L cannot be determined in a straightforward way, the total number of missing slides and missing landslide area is not calculated. Around one fifth of theoretical total number of landslides for Kabonero and Bundibugyo was mapped while the mapped landslide area covered over 50% of the theoretical total cover in the two study areas combined.

4.4. Landslide controlling factors

The distribution of slope angle, plan- and profile curvature and slope aspect for landslide depletion points and for the entire study areas are given in Figs. 6–8, respectively. A clear relation between slope steepness and the occurrence of landslides can be observed (Fig. 6). For plan- and profile curvatures and slope aspect, general relationships are much less evident (Figs. 7 and 8). These visual interpretations are supported by the χ^2-value and p-value for slope angle, slope aspect, profile- and plan curvature presented in Table 7. This-χ^2 test compares the distribution of landslides over different categorical classes represented in Figs. 6–9 over the distribution of that categorical class in the study area.

Fig. 9 represents the distribution of lithology over the study area and among the landslides for Kabonero and Bundibugyo. In Kabonero, the majority of slides occurs on soils developed on the dominant lithology (gneiss). In the amphibolite, very few slides occur while this lithology is present in 30% of the study area. There is a significant relationship between lithology and the occurrence of landslides in Kabonero (Table 7). Mahango is lithologically homogeneous: all slides occur on gneiss. In Bundibugyo most landslides were found in the rift alluvium which is also the largest lithological group in this study area (65%). In the field, the rift alluvium were observed to form very thick, clay-rich packages.

4.5. Landslide preparatory factors

Slope undercutting by erosional activity is a potential preparatory factor where the landslide toe reaches the river channel. In

Table 6
Comparison of the number and area of landslides mapped with the theoretically expected total number of landslides and total landslide area in Kabonero and Bundibugyo.

Study area	Number of landslides mapped	Theoretical number of landslides	% Landslides mapped	Area of landslides mapped	Theoretical total area of landslides	% Landslide area mapped
Kabonero	70	300	23%	0.40 km²	0.92 km²	43%
Bundibugyo	210	1000	21%	2.05 km²	3.07 km²	67%

Kabonero and Mahango, about one third of the slides were connected to a river. In Bundibugyo, nearly half of the slides are connected to a waterway (85 out of 194 landslides) i.e. 36% of the slides in the lowlands and 63% of slides in the highlands.

With regard to human-induced preparatory factors, deforestation is identified as a major issue for landslides in Africa (Davies, 1996; Broothaerts et al., 2012; Mugagga et al., 2012). Deforestation has been a continuous trend in East-Africa over the past two decades (Brink et al., 2014) and, in Uganda, it has been repeatedly identified as a key destabilizing factor in the Mount Elgon national park (Knapen et al., 2006). It could therefore be expected that the same trend occurs in the Rwenzori Mountains. However, in contrast to the Mount Elgon region, the park boundaries in the Rwenzori mountains are well respected and deforestation does not occur at a large scale. Despite a rough doubling of population densities in just more than two decades, deforestation has stopped at least from 2003 onwards due to the effective forest management and an increase in area for woodlots and tree plantations (Jagger and Shively, 2014; Jacobs et al., 2015).

Other human interventions such as the construction of roads and houses are known to destabilize slopes, especially in the Kabonero and Mahango study areas. Road network densities in Kabonero and Mahango are extremely low, however, in Kabonero, two newly constructed roads already show signs of instabilities (Fig. 10 A and C). In Mahango, the construction of houses was in particular an important preparatory factor. Slopes are often cut and subsequently overloaded to create a horizontal foundation. Similar construction methods are observed in other landslide-prone regions in Africa (e.g. Knapen et al., 2006; Che et al., 2011). The undercut slope is prone to failure which can cover portions of -or even entire-houses (Fig. 10 B). In the field, evidence of recent collapse of these earth walls were observed. In one case, this collapse occurred during the night, causing 5 fatalities as the failed wall covered the sleeping area of the children, traditionally sleeping in the upslope side of the house.

4.6. Landslide triggering factors

Rainfall and earthquakes are both main triggers of landslides in the Rwenzori (Jacobs et al., 2015). However, it is difficult to collect reliable data on the exact timing of landslides because there is little tradition of registering disastrous events by inhabitants or local
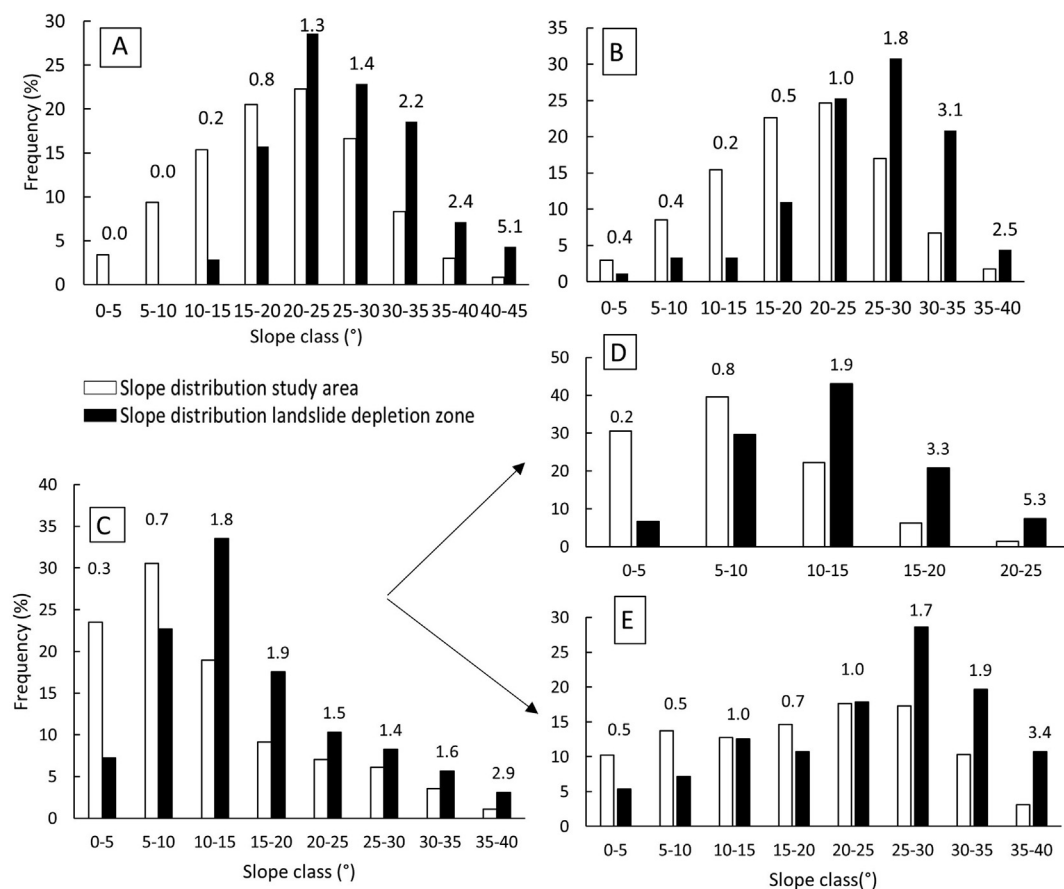

Fig. 6. Frequency distribution of slope angles for landslide depletion pixels (black bars) and all pixels in the study areas outside the landslide bodies (white bars). (A) Kabonero (n = 70), (B) Mahango (n = 91), (C) Bundibugyo (n = 194), (D) Bundibugyo lowlands (n = 135) and (E) Bundibugyo upland (n = 59). For each class, the corresponding FR is indicated.
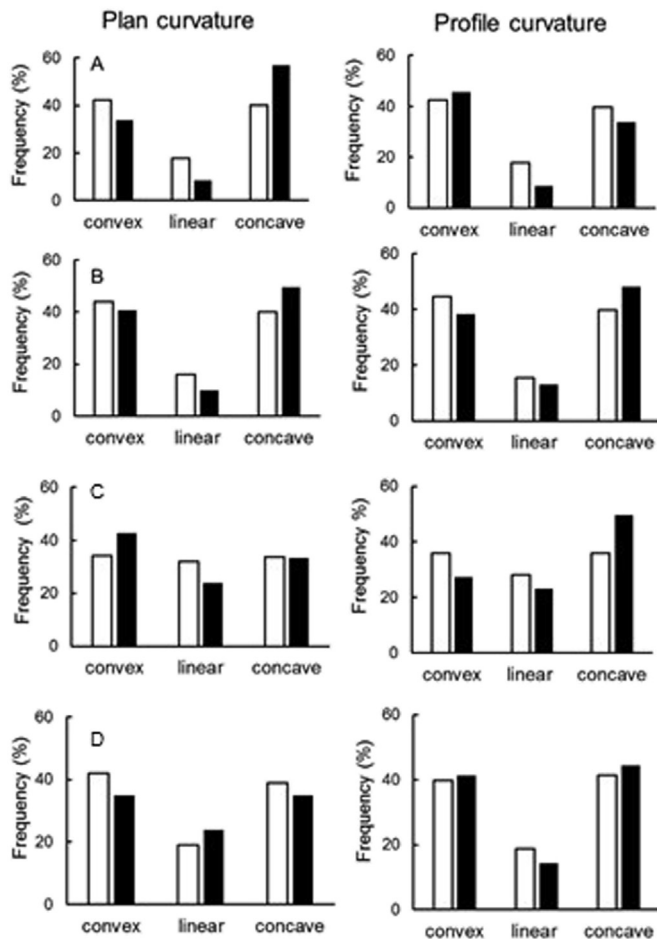
Fig. 7. Frequency distribution of plan curvature (Left) and profile curvature (Right) for landslide depletion pixels (black bars) and all pixels in the study areas outside the landslide bodies (white bars) (A) Kabonero (n = 70), (B) Mahango (n = 91), (C) Bundibugyo lowlands (n = 135), (D) Bundibugyo upland (n = 59).

Fig. 8. Frequency distribution of slope aspect for landslide depletion pixels (black line) and all pixels in the study areas outside the landslide bodies (grey line). (A) Kabonero (n = 70), (B) Mahango (n = 91), (C) Bundibugyo lowlands (n = 135), (D) Bundibugyo upland (n = 59).

administrations. Only for 262 (out of 371) landslides, the year of occurrence was reported and 202 out of these 255 slides have occurred after 2000. This is likely to represent a methodological bias due to a lack of registration of landslide events and therefore is not necessarily an indication for an increased landslide frequency in the past 15 years. The month of occurrence could be determined in 106 cases. Finally, for only 40 landslides the day of occurrence was known.

In contrast to the exact date of occurrence, inhabitants of landslide-affected areas generally do remember the triggering conditions for the landslide events. The vast majority of the landslides were reported to be triggered by rainfall (>95%). Their frequency of occurrence per month is given in Fig. 11. The very high number of landslides in May can be explained by one single event which occurred on the 1st of May 2013, triggering 30 landslides in the Mahango study area. Some of these landslides were reported in local newspapers, therefore the reported timing of the landslides can be verified. There was only one rainfall station operational in the vicinity of the study area at the period of this event. This tipping bucket rain gauge is located at 7.5 km north of the center of the Mahango study area at an altitude of 1500 m a.s.l.. The station has a temporal resolution of 24 h and measured a precipitation depth of 98 mm on the 1st of May 2013. Unfortunately, due to the limited registration of exact dates when landslides happen and the lack of rainfall stations in the Rwenzori Mountains, the establishment of
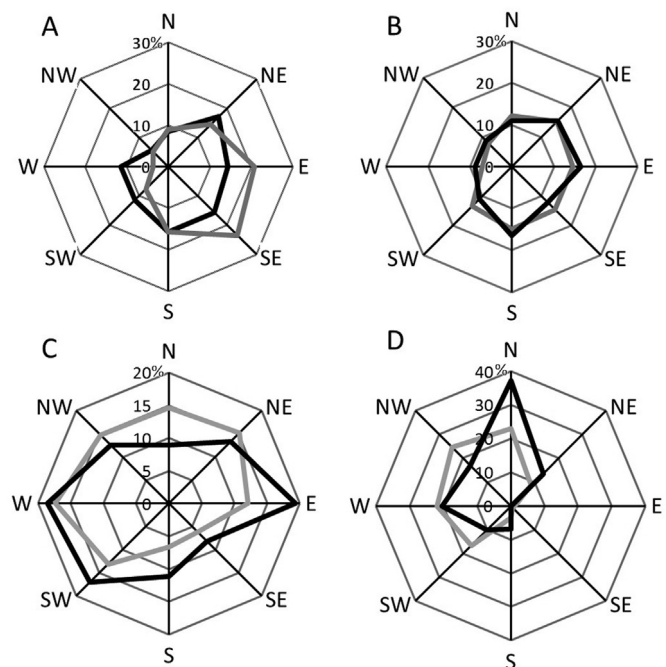
rainfall thresholds for landslide initiation is not possible based on this inventory.

In both Kabonero and Bundibugyo, six landslides were reported to be triggered by earthquake activity. In Mahango, none of the landslides were caused by earthquake activity according to the local population and guides. In Bundibugyo, one co-seismic landslide (area = 0.44 ha) occurred in the lowlands and is smaller than the average landslide size in rift alluvium (1.1 ha). In the highlands the co-seismic landslides are on average 0.84 ha which is larger than the average landslide sizes there (0.62 ha). In Kabonero the average size of co-seismic landslides is almost double (1.23 ha) of the average landslide size. An example of a co-seismic landslide in Kabonero is given in Fig. 12 (right). In both study areas the triggering earthquake events occurred in 1994 and 1966. These earthquakes are depicted in Fig. 12 (left) with their location, magnitude (USGS, 2015) and minimum and maximum zone of influence according to the following equation (Keefer, 2002):

$$\log_{10}A = M - 3.46(\pm 0.47) \tag{2}$$

where M is the moment magnitude of the earthquakes (between 5.5 and 9.2) and A the area (km^2) potentially affected by co-seismic slides. From this figure it is clear that Bundibugyo and Kabonero lie within the zone of influence of these earthquakes.

5. Discussion

5.1. Landslide characteristics and sliding mechanisms

The diversity of mass movements is large due to a variety of contrasting lithological, topographic, climatic and seismic conditions. In Kabonero and Mahango which are similar in terms of lithology and topography, landslide types, processes, densities and dimensions are very similar. Landslide densities are quite low, and shallow translational soil slides with average areas between 0.3 and

Table 7
χ^2-values and associated p-values for slope, aspect, plan curvature and profile curvature (*confidence level = 0.95, **confidence level = 0.99). (NA. = not applicable).

	Kabonero	Mahango	Bundibugyo lowlands	Bundibugyo upland
Slope angle	31.9 ($<8 \times 10^{-4}$)**	27.7 ($<4 \times 10^{-3}$)**	31.3 ($<1 \times 10^{-5}$)**	12.9 (0.114)
Aspect	7.6 (0.366)	0.9 (0.996)	4.8 (0.690)	10.5 (0.161)
Plan curvature	7.2 (0.028)*	2.5 (0.287)	2.5 (0.281)	0.85 (0.653)
Profile curvature	3.1 (0.213)	1.5 (0.478)	4.9 (0.086)	1.1 (0.567)
Lithology	31.1 ($<2 \times 10^{-7}$)**	NA	1.2 (0.547)	

0.6 ha prevail. This contrasts to the Bundibugyo study area, which is very heterogeneous in nature, both topographically and lithologically. In this region there is a large contrast between the less steep lowlands in the rift alluvium and the steep highlands under mica schists and gneiss. In the uplands, shallow translational soil and debris slides dominate while in the lowlands, where most landslides were mapped, deep rotational soil slides are by far the most common (Table 4). The landslides in the Bundibugyo lowlands, with an average scarp depth of 9 m and landslide area of nearly 1.1 ha, differ significantly from the landslides found in the uplands of Bundibugyo, Mahango and Kabonero (Fig. 4). This is explained by the presence of deep soil profiles and loose, clay-rich sediment deposits, prone to sliding. Finally, in Bundibugyo the landslides showed more signs of instability and recent activity than in Mahango or Kabonero.

5.2. Interpretation of the landslide frequency-size analysis

The most striking feature is an underrepresentation of landslides of small sizes (<1.5 ha) (Fig. 5). The inventories presented here are not connected to one specific triggering event and their date of origin can differ decades in time. Landslides that were masked by tillage- and water erosion, reclaimed by agriculture or recolonized by vegetation at the time of observation are not represented. This masking will mostly affect small landslides. The difficulties associated with identifying smaller landslides occurring within a larger landslide body can reinforce this underrepresentation. Very large landslides will remain visible in the field for a longer period of time implying that they are more likely to be nearly completely represented in the inventory. This is confirmed by the good fit of frequency distributions for landslides above 1.5 ha for which decay coefficients ($\rho + 1$ in Eq. (1)) of 1.9 and 2.2 were found in Kabonero and Bundibugyo respectively. These values fall well within the range of values that are found in the literature (Van Den Eeckhaut et al., 2007). In a similar context where only landslide areas above 2 ha were considered, Van den Eeckhaut et al. (2007) found a decay coefficients of 2.3 for their historical inventory. In Bundibugyo, the proposed decay coefficient of 2.4 by Malamud et al. (2004) is best approached. This is considered to be a result of the fact that the deep-seated rotational landslides in Bundibugyo with areas above 1.5 ha are less easily erased by soil erosion, sediment deposition, natural vegetation or land levelling for agriculture. Therefore they have a more complete representation in the inventories.

Despite the underrepresentation of smaller landslides, the rates of completeness shown in Table 6 are similar to or outperform other examples of historical inventories (e.g. Malamud et al., 2004; Van Den Eeckhaut et al., 2007; Guzzetti et al., 2008). Due to fast vegetation regrowth, frequent cloud cover and the limited availability of remote sensing data, the identification of landslides on satellite images or aerial photographs would not allow reaching such high degrees of completeness.

5.3. Controlling factors

The slope angle is a primary control for the occurrence of especially shallow landslides (Sidle and Ochiai, 2006; van Westen et al., 2008). Indeed, for the three study areas, Fig. 6 shows that slope angle is a determining factor explaining the spatial distribution of landslides. This is confirmed by a significant influence of slope angle for the occurrence of landslides in Kabonero, Mahango and the lowlands of Bundibugyo represented in Table 7. Sidle and Ochiai (2006) report that slopes above 25° are potentially subject to landslides especially where the soil mantle is not well bound to the underlying rocks while above 35°, most slopes are subject to any type of landslides. This is also observed in the upland regions (Kabonero, Mahango and the uplands of Bundibugyo) where the highest FRs for slope angle are found for slope angles above 25°. In the Bundibugyo lowlands, slope angles are in general much lower, and landslides concentrate on slopes above 10−15°. This is comparable to slope angles susceptible to landslides in similar lowland regions with clay-rich soils and subsoils (e.g. Ost et al., 2003).

Profile curvature determines the driving and resisting forces in the direction of a potential slide while plan curvature determines the concentration of soil moisture and landslide material in plan-concave sections and the potential for the development of perched water tables (Ohlmacher, 2007; Sidle and Ochiai, 2006). As such, plan- and profile-concave slopes are generally found to be most likely to fail in case of rainfall-triggered landslides.
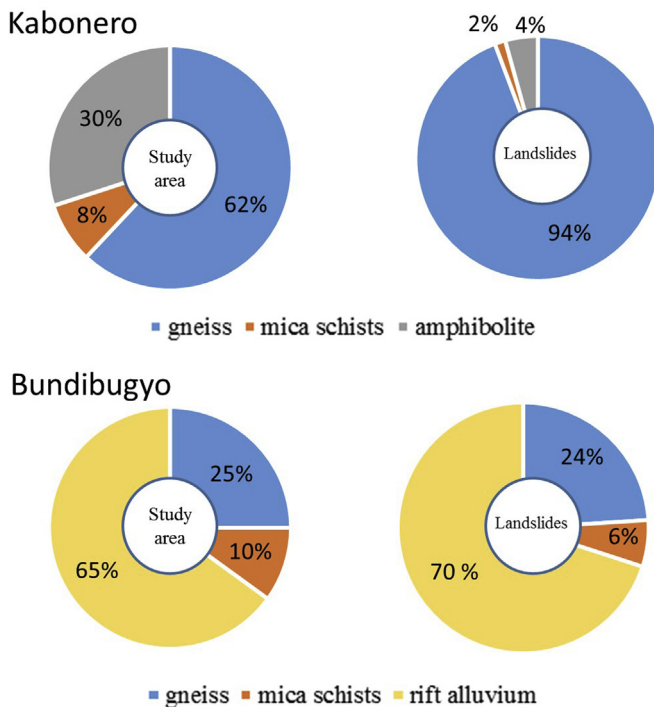

Fig. 9. Distribution of each lithological class over the study area (left) and landslides (right) expressed as a % of the study area or landslide area covered by the lithological unit.

Fig. 10. Failures along a newly constructed road (Kabonero, October 2014) (A, C), Failure of a cut in the hillslope for the construction of a house (Mahango, September 2014) (B).

Nevertheless, this is only observable in Mahango (Fig. 7) and these relations are not statistically significant (Table 7). In Kabonero, the occurrence of landslides is only strongly connected to plan-concave slopes and statistically significant while in Bundibugyo there is a concentration of landslides in profile concavities in the lowlands (Fig. 7) but no significant relationships between the occurrence of landslides and slope curvatures were found. Curvature is derived from a 30 m resolution DEM. For the calculation of curvature in a certain direction, three pixels are necessary. Given that for 75% of all landslides, the width is below three pixels (90 m), these weak signatures between curvature and the occurrence of landslides can be explained by the coarse resolution of the DEM. This limitation of DEM resolution is confirmed by field observations where landslides are often found in local topographic hollows.

With regard to hillslope aspect, it seems that landslides occur less on south-east-slopes in Kabonero, less on north-slopes in the lowlands of Bundibugyo and more on north-facing slopes in the Bundibugyo uplands (Fig. 8). However, no significant relations could be found (Table 7). This could indicate that spatial rainfall patterns do not vary significantly with slope aspect.

With regard to the control of lithology, two conclusions can be drawn. Firstly, in the clay-rich rift alluvium, the density of landslides is the highest in the entire sampled area of the Rwenzori region despite the modest relief of these lowlands. Secondly, in Kabonero, the amphibolites seem to have a stabilizing effect on slopes, with only relatively few landslides observed. This can be explained by its high friction angle compared to gneiss or schists (Barton and Choubey, 1977). The reported approximate friction angle for gneiss is reported to range between 23 and 29° (Barton and Choubey, 1977). This corresponds to the range of slope angles where landslides concentrate in the study areas dominated by gneiss.

5.4. Preparatory factors

Undercutting of hillslopes by river erosion is expected to be an important natural preparatory factor for landslide occurrence. Especially in Bundibugyo, slope undercutting by a river is expected to play a role in slope destabilization. Here, the width to length ratio is higher than in Mahango and Kabonero and relatively more landslides are linked to the river channel. The anthropogenic influence on the occurrence of landslides is limited when only considering the number of affected landslides. However, although few in number, the landslides where undercutting of the slope for house construction was an important preparatory factor, were found to cause several fatalities.
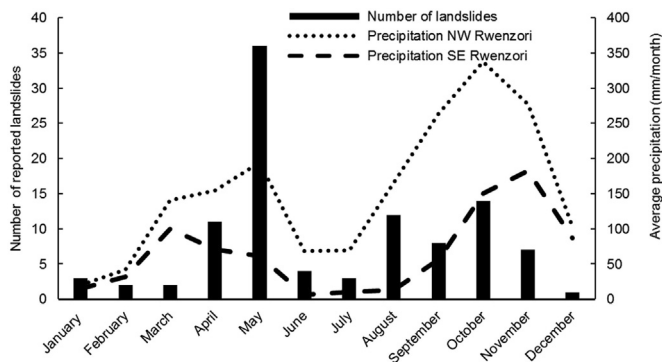

Fig. 11. Number of reported landslides per month from 1990 to 2015 for all study areas (n = 103) combined together with the average monthly precipitation in the NW and SE Rwenzori as modelled by Thiery et al. (2015). Details about the modeling procedure can be found in Jacobs et al. (2015).
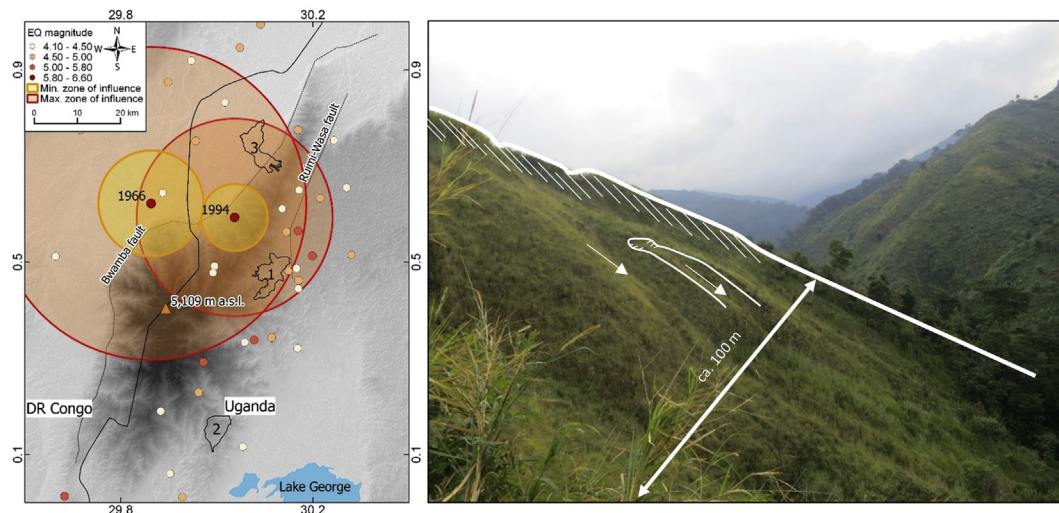
Fig. 12. Left: Dots indicate location of earthquakes (EQ) between 1900 and 2015 with M > 4 according to USGS (2015) together with the minimal and maximum zone of influence of the two most recent earthquakes with Mw > 5.5 (1966 and 1994) according to eq. (2). 1 = Kabonero study area, 2 = Mahango study area, 3 = Bundibugyo study area. Right: Illustration of a co-seismic landslide in Kabonero triggered in 1994 (August 2014).

5.5. Triggering factors

Rainfall is by far the main triggering factor for landslides in the Rwenzori, though strong earthquakes (Mw > 6) have also triggered landslides in the Bundibugyo and Kabonero and other regions in the Rwenzori (Jacobs et al., 2015). The areas where co-seismic landslides were found in the field correspond well to the predicted zones of influence of the two last major earthquakes according to the equation proposed by Keefer (2002). It is observed that in the Mahango study area, which falls completely outside of these zones, no co-seismic landslides were reported.

Since there are almost no operational rainfall stations in the Rwenzori Mountains between 1000 and 2300 m a.s.l. (the elevation range of the study areas and in general of the inhabited region of the mountain range) and due to the lack of any registration of landslide events by local authorities, the construction of empirical rainfall thresholds was not possible. During one single event, a rainfall amount of nearly 100 mm per day has triggered 30 landslides in Mahango sub-county and several others in neighboring catchments (Jacobs et al., under revision).

6. Conclusions

A comprehensive field survey in three regions of the Rwenzori Mountains resulted in a field inventory with 371 landslides mapped in detail. Landslide processes depend largely on the prevailing lithology. There is a dominance of shallow translational soil slides on gneiss lithology and deep rotational soil slides in the rift alluvium of the lowlands. Slope angle is the main controlling topographic factor for landslides. No clear relation with aspect nor plan or profile curvature exists. Most of the landslides are triggered by rainfall but co-seismic landslides were also found within the zone of influence of the Mw > 6 1966 and 1994 earthquakes.

In this region and similar environments where vegetation regrowth and reclamation by agriculture hamper the identification of landslides on aerial photographs or satellite images, field surveys including communication with local inhabitants are indispensable. Although time-consuming, they allow to describe in detail the geomorphological process. In addition, they do not require remote sensing images, difficult to obtain in humid, cloud-rich environments.

In order to facilitate landslide hazard assessment, proper registration of timing and location of new events by local authorities and detailed monitoring of triggering events (both high spatial and temporal resolution rainfall data as well as earthquake activity) is essential. These monitoring systems serve the final goal of establishing an early warning system and are therefore strongly recommended.

References

Ayalew, L., 1999. The effect of seasonal rainfall on landslides in the highlands of Ethiopia. Bull. Eng. Geol. Environ. 58, 9—19. http://dx.doi.org/10.1007/s100640050065.

Barton, N.R., Choubey, V., 1977. The shear strength of rock fractures in theory and practice. Rock Mech. 10, 1—54.

Brink, A.B., Bodart, C., Brodsky, L., Defourney, P., Ernst, C., Donney, F., Lupi, A., Tuckova, K., 2014. Anthropogenic pressure in East Africa—Monitoring 20 years of land cover changes by means of medium resolution satellite data. Int. J. Appl. Earth Obs. Geoinf 28, 60—69. http://dx.doi.org/10.1016/j.jag.2013.11.006.

Broothaerts, N., Kissi, E., Poesen, J., Van Rompaey, a., Getahun, K., Van Ranst, E., Diels, J., 2012. Spatial patterns, causes and consequences of landslides in the Gilgel Gibe catchment, SW Ethiopia. Catena 97, 127—136. http://dx.doi.org/10.1016/j.catena.2012.05.011.

Che, V.B., Kervyn, M., Ernst, G.G.J., Trefois, P., Ayonghe, S., Jacobs, P., Van Ranst, E., Suh, S.E., 2011. Systematic documentation of landslide events in Limbe area (Mt Cameroon Volcano, SW Cameroon): geometry, controlling, and triggering factors. Nat. Hazards 59, 47—74. http://dx.doi.org/10.1007/s11069-011-9738-3.

Crozier, M.J., Glade, T., 2005. Chapter 1: landslide hazard and risk: issues, concepts, and approach. In: Thomas, G., Anderson, M., Crozier, M.J. (Eds.), Landslide Hazard and Risk. John Wiley & Sons Ltd, London, pp. 1—34.

Cruden, D., Varnes, D., 1996. Landslide types and processes. In: Turner, A., Schuster, R. (Eds.), Landslides: Investigation and Mitigation. Transportation Research Board, National Research Council, vol. 247, pp. 36—75.

Davies, T.C., 1996. Landslide research in Kenya. J. Afr. Earth Sci. 23, 541—545.

Dewitte, O., Chung, C.-J., Cornet, Y., Daoudi, M., Demoulin, A., 2010. Combining spatial data in landslide reactivation susceptibility mapping: a likelihood ratio-based approach in W Belgium. Geomorphology 122, 153–166. http://dx.doi.org/10.1016/j.geomorph.2010.06.010.

FAO, 2003. Mulitpurpose Landcover Database of Uganda-Africover. http://www.fao.org/geonetwork/srv/en/metadata.show?id=38103&currTab=simple [on line] Accessed 22th March 2015.

Glade, T., Crozier, M.J., 2005. Chapter 2: the nature of landslide hazard impact. In: Thomas, G., Anderson, M., Crozier, M.J. (Eds.), Landslide Hazard and Risk. John Wiley & Sons Ltd, London, pp. 35–61.

Goetz, J.N., Guthrie, R.H., Brenning, A., 2015. Forest harvesting is associated with increased landslide activity during an extreme rainstorm on Vancouver Island, Canada. Nat. Hazards Earth Syst. Sci. 15, 1311–1330. http://dx.doi.org/10.5194/nhess-15-1311-2015.

Google Earth, 2015. Rwenzori Mountains 30°E, 0.5°N. http://www.earth.google.com [on line] Accessed 15th June 2015.

GTK Consortium, 2012. Geological Map of Uganda 1:100,000 Sheet N° 65 Karambi.

Guzzetti, F., Ardizzone, F., Cardinali, M., Galli, M., Reichenbach, P., Rossi, M., 2008. Distribution of landslides in the upper tiber river basin, central Italy. Geomorphology 96, 105–122. http://dx.doi.org/10.1016/j.geomorph.2007.07.015.

Guzzetti, F., Mondini, A.C., Cardinali, M., Fiorucci, F., Santangelo, M., Chang, K.T., 2012. Landslide inventory maps: new tools for an old problem. Earth-Science Rev. 112, 42–66. http://dx.doi.org/10.1016/j.earscirev.2012.02.001.

Hungr, O., Leroueil, S., Picarelli, L., 2014. The Varnes classification of landslide types, an update. Landslides 11, 167–194. http://dx.doi.org/10.1007/s10346-013-0436-y.

Jacobs, L., Dewitte, O., Poesen, J., Delvaux, D., Thiery, W., Kervyn, M., 2015. The Rwenzori Mountains, a Landslide-prone Region? Landslides. http://dx.doi.org/10.1007/s10346-015-0582-5.

Jacobs L., Maes J., Mertens K., Sekajugo J., Thiery W., van Lipzig N., Poesen J., Kervyn M., and Dewitte O., Reconstruction of a Flash Flood Event through a Multi-hazard Approach: Focus on the Rwenzori Mountains, Uganda. Natural Hazards under revision.

Jagger, P., Shively, G., 2014. Land use change, fuel use and respiratory health in Uganda. Energy Policy 67, 713–726. http://dx.doi.org/10.1016/j.enpol.2013.11.068.

Keefer, D.K., 2002. Investigating landslides caused by earthquakes- a historical review. Surv. Geophys. 23, 473–510.

Kervyn, M., Jacobs, L., Maes, J., Che, V.B., de Hontheim, A., Dewitte, O., Isabirye, M., Sekajugo, J., Kabeseke, C., Poesen, J., Vranken, L., Mertens, K., 2015. Landslides resilience in Equatorial Africa: moving beyond the problem identification! Belg. J. Geogr. 1–2015.

Knapen, A., Kitutu, M.G., Poesen, J., Breugelmans, W., Deckers, J., Muwanga, A., 2006. Landslides in a densely populated county at the footslopes of Mount Elgon (Uganda): characteristics and causal factors. Geomorphology 73, 149–165. http://dx.doi.org/10.1016/j.geomorph.2005.07.004.

Lee, S., Pradhan, B., 2007. Landslide hazard mapping at Selangor, Malaysia using frequency ratio and logistic regression models. Landslides 4, 33–41. http://dx.doi.org/10.1007/s10346-006-0047-y.

Lindenfeld, M., Rümpker, G., Batte, A., Schumann, A., 2012. Seismicity from february 2006 to september 2007 at the Rwenzori mountains, East African rift: earthquake distribution, magnitudes and source mechanisms. Solid Earth 3, 251–264. http://dx.doi.org/10.5194/se-3-251-2012.

Maes, J., Kervyn, M., de Hontheim, A., Dewitte, O., Jacobs, L., Mertens, K., Vanmaercke, M., Vranken, L., Poesen, J., 2016. Landslide Risk Reduction Strategies: a Review of Practices and Challenges for the Tropics. Progress in Physical Geography accepted with revision.

Maki Mateso, J.-C., Dewitte, O., 2014. Towards an inventory of landslide processes and the elements at risk on the Rift flanks West of Lake Kivu (DRC). Geo-Eco-Trop 38, 137–154.

Malamud, B.D., Turcotte, D.L., Guzzetti, F., Reichenbach, P., 2004. Landslide inventories and their statistical properties. Earth Surf. Process. Landforms 29, 687–711. http://dx.doi.org/10.1002/esp.1064.

Mertens, K., Jacobs, L., Maes, J., Kabaseke, C., Maertens, M., Poesen, J., Kervyn, M., Vranken, L., 2016. The direct impact of landslides on household income in tropical regions: a case study on the Rwenzori Mountains in Uganda. Sci. Total Environ 550, 1032–1043. http://dx.doi.org/10.1016/j.scitotenv.2016.01.171.

Mugagga, F., Kakembo, V., Buyinza, M., 2012. Land use changes on the slopes of Mount Elgon and the implications for the occurrence of landslides. Catena 90, 39–46. http://dx.doi.org/10.1016/j.catena.2011.11.004.

Ngecu, W.M., Ichang'i, D.W., 1999. The environmental impact of landslides on the population living on the eastern foot slopes of the Aberdare ranges in Kenya: a case study of Maringa Village landslide. Environ. Geol. 38, 259–264.

Ohlmacher, G.C., 2007. Plan curvature and landslide probability in regions dominated by earth flows and earth slides. Eng. Geol. 91, 117–134. http://dx.doi.org/10.1016/j.enggeo.2007.01.005.

Ost, L., Van Den Eeckhaut, M., Poesen, J., Vanmaercke-Gottigny, M.C., Lieven, Ost, Miet Van Den Eeckhaut, J.P., M.C.V.-G, 2003. Characteristics and spatial distribution of large landslides in the Flemish Ardennes (Belgium). Z. fur Geomorphol. N. F. 47, 329–350.

Sidle, R.C., Ochiai, H., 2006. Landslides: Processes, Prediction, and Land Use, Water Resources Monograph. American Geophysical Union, Washington, D. C. http://dx.doi.org/10.1029/WM018.

Stark, C.P., Hovius, N., 2001. The characterization of landslide size distributions. Geophys. Res. Lett. 28, 1091–1094. http://dx.doi.org/10.1029/2000GL00852.

Thiery, W., Davin, E., Panits, H.-J., Demuzere, M., Lhermitte, S., Van Lipzig, N., 2015. The impact of the African Great Lakes on the regional climate. J. Clim. 28, 4061–4085. http://dx.doi.org/10.1175/JCLI-D-14-00565.1.

USGS, 2014. Shuttle Radar Topography Mission, 1 Arc Second Scenes SRTM1N00E030V3, SRTM1N00E029V3, SRTM1S01E030V3, SRTM1S01E029V3, Unfilled Unfinished. Global Land Cover Facility, University of Maryland, College Park, Maryland. February 2000.

USGS, 2015. Earthquake Archives. http://earthquake.usgs.gov/earthquakes/search/ [on line] Accessed 31th July 2015.

Van Den Eeckhaut, M., Vanwalleghem, T., Poesen, J., Govers, G., Verstraeten, G., Vandekerckhove, L., 2006. Prediction of landslide susceptibility using rare events logistic regression: a case-study in the Flemish Ardennes (Belgium). Geomorphology 76 (3), 392–410.

Van Den Eeckhaut, M., Poesen, J., Govers, G., Verstraeten, G., Demoulin, a, 2007. Characteristics of the size distribution of recent and historical landslides in a populated hilly region. Earth Planet. Sci. Lett. 256, 588–603. http://dx.doi.org/10.1016/j.epsl.2007.01.040.

Van Den Eeckhaut, M., Moeyersons, J., Nyssen, J., Abraha, A., Poesen, J., Haile, M., Deckers, J., 2009. Spatial patterns of old, deep-seated landslides: a case-study in the northern Ethiopian highlands. Geomorphology 105, 239–252. http://dx.doi.org/10.1016/j.geomorph.2008.09.027.

Van Westen, C.J., Castellanos, E., Kuriakose, S.L., 2008. Spatial data for landslide susceptibility, hazard, and vulnerability assessment: an overview. Eng. Geol. 102, 112–131. http://dx.doi.org/10.1016/j.enggeo.2008.03.010.

Zogning, A., Ngouanet, C., Tiafack, O., 2007. The catastrophic geomorphological processes in humid tropical Africa: a case study of the recent landslide disasters in Cameroon. Sediment. Geol. 199, 13–27. http://dx.doi.org/10.1016/j.sedgeo.2006.03.030.